METHOD OF CHARACTERISTICS VERIFICATION OF INVERSE FREQUENCY MODEL OF TURBULENT PIPE FLOW TRANSIENTS.

By

Mohammad Saifullah Mohammad Zafar Shaikh

Presented to the Faculty of the Graduate School of

The University of Texas at Arlington

In Fulfillment of the Requirements

for the Degree of

MASTER OF SCIENCE IN

MECHANICAL ENGINEERING

THE UNIVERSITY OF TEXAS AT ARLINGTON

May 2016

Acknowledgements

I take this opportunity to express my sincere thanks to Professor Hullender, my supervising professor, for providing me with all the valuable instructions on the course of my thesis.

May 6, 2016

Dedication

This thesis is dedicated to Mr. Mohammad Zafar Shaikh -my father who made me realize the statement “A father’s best and greatest gift to child is education”, Mrs. Naseemakhtar Shaikh-My mother who taught me never to give up by setting herself a living example.

I would also love to dedicate this thesis to my Beautiful sisters Ms. Humeyra Shaikh and Mrs. Ayesha Shaikh who provided me an emotional and mental support.

And My friends Atul Mohandas, Ninad kawle, Umang Dighe, Adeetya Ravisankar,Sudheer Barkham,Samruddhi Deokar and Sandip Patil for always supporting, being there for me and providing me the crucial help.

Abstract

METHOD OF CHARACTERISTICS VERIFICATION OF

INVERSE FREQUENCY MODEL OF

TURBULENT PIPE FLOW

TRANSIENTS.

Mohammad Saifullah Mohammad Zafar Shaikh, M.S.

The University of Texas at Arlington, 2016

Supervising Professor: David Hullender

Pressure transients in pipes with turbulent flow have classically been simulated using numerical techniques such as the method of characteristics. An alternative method utilizing an inverse frequency algorithm has recently been introduced for smooth pipe and determined to be computationally fast compared to the method of characteristics and in some cases more accurate. In addition, comparisons with experimental water hammer data has verified that the inverse frequency method is accurate out to Reynolds numbers of 15,800. This thesis investigates a comparison or the inverse frequency and method of characteristics methods for Reynolds numbers out to 200,000 for smooth pipes.

Table of Contents

List of Illustrations

List of Tables

Chapter 1

Introduction

Water hammer is a phenomenon where a pressure surge in a line is caused when the motion of fluid is stopped or its direction is suddenly changed such as in blood circulation systems, industrial fluid systems, etc. The effects of such pressure surges may cause damage to a pipe or line and hence it is of interest to study this problem.

Many researchers have studied and analyzed the water hammer problem using various approximation methods. For turbulent flow, the method of characteristics (MOC) gives reasonably accurate solutions depending on the complexity of the nonlinear interaction of friction and interpolation errors; the accuracy is very dependent on the assumed grid size when spacing the nodes. For the MOC method, the unsteady frictional head loss term in the momentum partial differential equation is approximated. This unsteady frictional head loss term has been calculated and verified experimentally by different researchers [4-13] based on various assumed boundary conditions for relatively low Reynolds numbers on the order of 15,800. However, an alternate approach based on an inverse frequency algorithm [1] has been formulated that provides more flexibility with the boundary conditions corresponding to potential applications other than the water hammer problem.

The Inverse frequency model [1] has been proven to provide computationally fast and provide good agreement with experimental data for smooth pipes and Reynolds numbers out to about 15,800. However, the friction factor empirical model used in the formulation is normally limited to Reynolds numbers on the order of 100,000. Of significant interest is the potential use of the inverse frequency model for Reynolds numbers greater than 15,800 for smooth pipe; additional experimental data is needed for verification at higher Reynolds numbers. Although the MOC method is also unproven at higher Reynolds numbers, the focus of this thesis is a theoretical comparison of the MOC and the inverse frequency methods at higher Reynolds numbers for smooth pipe.

Chapter 2

Model Based on Method of Characteristics.

Method of characteristics (MOC) is a numerical method used to solve partial differential equations by formulating lines, (generally referred as characteristic curves or characteristics) along which the partial differential equations are transformed to ordinary differential equations. In this study this numerical method is used to solve the water hammer problem [11].

$$\frac{\partial p}{\partial t} + \rho a^2 \frac{\partial V}{\partial x} = 0 \quad (1)$$

$$\frac{1}{\rho}\frac{\partial p}{\partial x} + \frac{\partial V}{\partial t} + H_f = 0 \quad (2)$$

The equations of motion (1) and continuity (2) are integrated along the lines. These characteristic lines represent the motion of waves travelling at the wave speed in both directions along a pipe. The solution of equations (1) and (2) using the MOC is shown below.

Using equation (1) and (2) and adding a Lagrange multiplier λ

$$\lambda\left\{\frac{dV}{dt} + \frac{1}{\rho}\frac{\partial p}{\partial x} + H_f\right\} + \lambda\left\{\rho a^2 \frac{\partial V}{\partial x} + \frac{dp}{dt}\right\} = 0 \quad (3)$$

Gathering Terms:

$$\left(\lambda \frac{dV}{dt} + \rho a^2 \frac{\partial V}{\partial x}\right) + \left(\frac{\lambda}{\rho}\frac{\partial p}{\partial x} + \frac{\partial p}{\partial t}\right) + \lambda H_f = 0 \quad (4)$$

Now

$$\lambda \frac{dV(x,t)}{dt} = \lambda \frac{\partial V}{\partial t} + \lambda \frac{\partial V}{\partial x}\frac{dx}{dt} \quad (5)$$

By comparing with the first terms in equation (4), leads to the following

$$\lambda \frac{dx}{dt} = \rho a^2 \quad (6)$$

Again

$$\frac{dp(x,t)}{dt} = \frac{\partial p}{\partial x}\frac{dx}{dt} + \frac{\partial p}{\partial t} \quad (7)$$

Comparing with the second term in equation (4), leads to the following

$$\frac{\lambda}{\rho} = \frac{dx}{dt} \quad (8)$$

$$\lambda . \frac{\lambda}{\rho} = \rho a^2 \quad (9)$$

Therefore

$$\lambda = \pm \rho a \quad (10)$$

Hence substituting λ in equation (4) will lead to positive and negative characteristics depending on the substitution. For the positive characteristics

$$\frac{dV}{dt} + \frac{1}{\rho a}\frac{dp}{dt} + H_f = 0 \quad (11)$$

For the negative characteristics

$$\frac{dV}{dt} - \frac{1}{\rho a}\frac{dp}{dt} + H_f = 0 \quad (12)$$

Using equations (8) and (10), we get

$$\frac{dx}{dt} = \pm a \quad (13)$$

For positive characteristics,

$$x = at + c$$

$$t = \frac{x}{a} - \frac{c}{a} \quad (14)$$

Similarly, for negative characteristics

$$t = \frac{x}{a} - \frac{c}{a} \quad (15)$$

Equations (14) and (15) represent straight line relations, which helps to generate the following diagram.

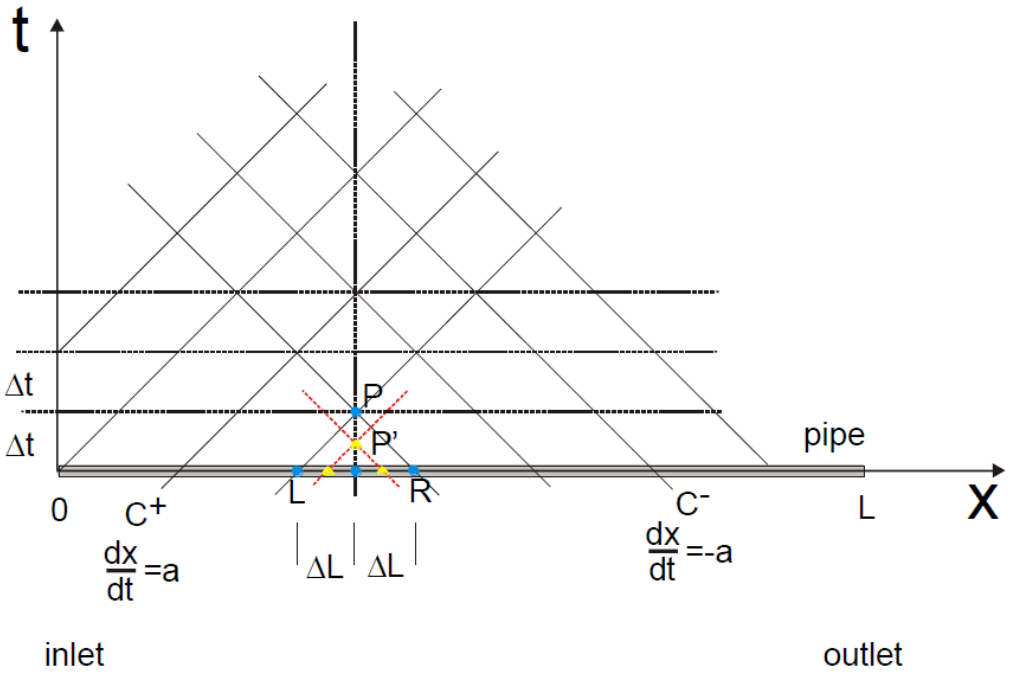

Figure 1. Method of characteristics grid

In the past years the greatest challenge with the water hammer problem is the calculation of the friction coefficient in turbulent flow modelling. Although the steady-state friction component is well defined, the unsteady friction component can only be approximated for time-domain simulations. It was initially Zielke [4] who provided a proposed reasonably accurate solution, but at the expense of a very high computational load.

$$H_f = \frac{f}{2D} V(t)|V(t)| + \frac{16\nu}{D^2}\int_0^t W_0(t-t^*) \qquad (16)$$

Then Trikha [10] and Kagawa et al. [11] later evaluated weighting factors to simplify computations for a series of unsteady friction terms. Later Vitkovsky et al [12]

developed a more efficient and accurate model for turbulent flow modeling based on Vardy and Brown's model [8]. Although, there are many models that came after the Vitkovsky model, his model is very popular for calculating the unsteady turbulent friction term because of its simplicity.

$$H_f = \frac{f}{2D} V(t)|V(t)| + \frac{16\nu}{D^2}\sum_{k=1}^{N} y_k(t) \quad (17)$$

Where

$$y_k(t) = \int_0^t \frac{\partial V}{\partial t} m_k e^{-n_k K(t-t^*)} dt^* \quad (18)$$

Which is further approximated and modified to [12]

$$y_k(t+2\Delta t) = e^{-n_k \Delta\tau}\{e^{-n_k \Delta\tau} y_k(t) + m_k[V(t+2\Delta t) - V(t)]\} \quad (19)$$

Where

$$m_k = A * m_k^* \text{ And } n_k = B + n_k^* \quad (20)$$

In equation (20), m_k and n_k are scaling coefficients in terms of A and B which are defined below as equation (21) for rough pipe in general.

$$A = 0.0103\sqrt{Re}\left(\frac{\epsilon}{D}\right)^{0.39} \text{ And } B = 0.352Re\left(\frac{\epsilon}{D}\right)^{0.41} \quad (21)$$

Equations (21) and (22) define the coefficients for rough and smooth pipes respectively.

$$A = \frac{1}{2\sqrt{\pi}}, \quad B = \frac{Re^k}{12.86} \text{ and } \quad k = \log_{10}(15.29\, Re^{-0.0567}) \quad (22)$$

$$\Delta\tau = \frac{4\nu\Delta t}{D^2} \tag{23}$$

In Chapters 3 and 4, results obtained by using equations (11), (12) and (17) are discussed.

Chapter 3

Overview of inverse frequency model and its comparison with method of charecteristics at lower Reynolds numbers

Inverse Frequency Model: In contrast to previous approaches for modeling turbulence by modifying the head loss terms in the momentum partial differential equation, the inverse frequency approach is achieved by coupling the frequency domain analytical solution to the laminar flow version of the partial differential equations in series with a lumped resistance that has been sized so that the steady flow resistance for the line is equivalent to an empirical turbulent steady flow resistance [1]. This model has been proven to give accurate results for Reynolds numbers up to 15800 [1]; experimental data is needed for verification at higher Reynolds numbers.

For all the comparisons shown in this thesis, n represents number of line segments used in the inverse frequency model. A line segment consists of a hypothetical portion of the line with laminar flow coupled with a steady flow resistance to achieve the correct steady flow for turbulence for that segment. For example, if n = 2, the length of each segment is L/2 where L is the total line length. A simulation model was created using the MOC; the unsteady turbulent friction term in the momentum equation was calculated using the weighing function coefficients given by Vitkovosky et.al [12].

For all the comparisons in this thesis, the number of nodes used in the model is 100. The number of nodes can be increased further to get better accuracy but at the expense of increased computation time.

The first comparison is shown in Figure. 2 for a pipe with length 177.4 m. The parameters correspond to experimental apparatus in [7].

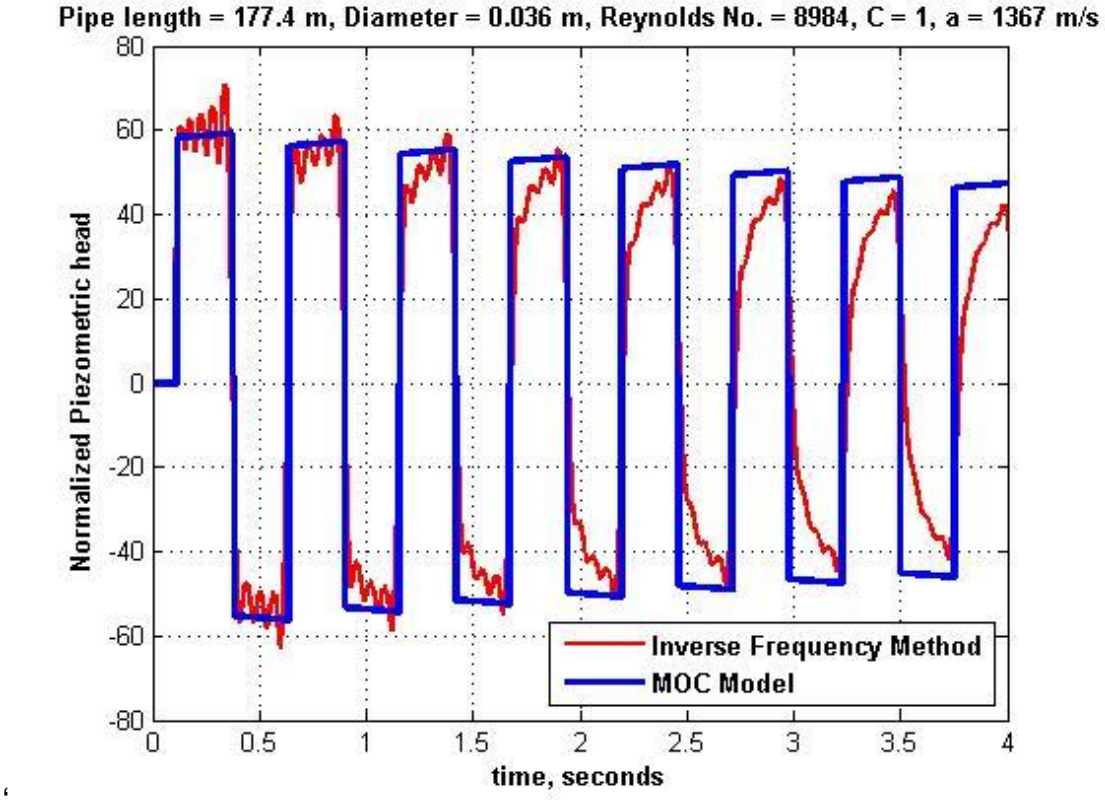

Figure 2. Comparing the response of the inverse frequency model with the MOC response for pipe length 177.4 m, diameter 0.036 m, Reynolds No. 8984, and wave velocity of 1367 m/s and valve closing time of 0.02 sec

As demonstrated in [1], the inverse frequency response agrees very well with the experimental data in [7]. However in Fig. 2, it is obvious that the MOC grid size is too large to model the higher frequencies; however, of prime importance is the comparison of the response decay rate and the primary mode frequency which agree quite well.

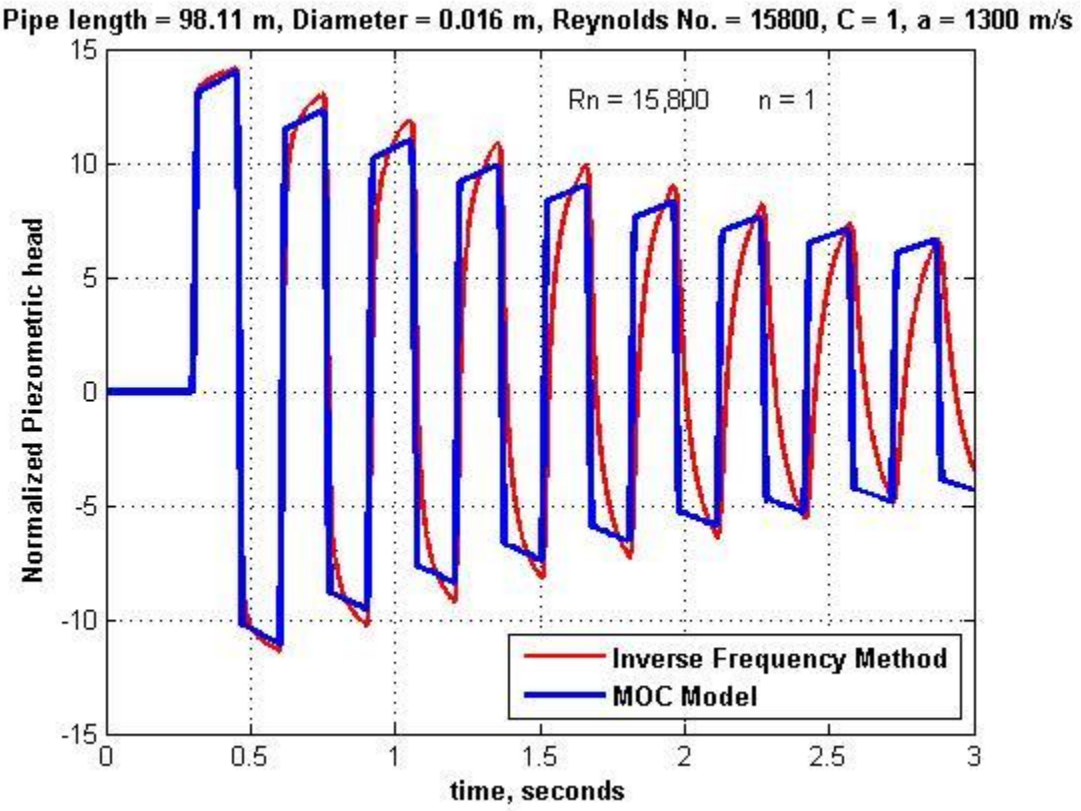

Figure 3. Comparing the response of the inverse frequency model [1] with the MOC response for pipe length 98.11 m, diameter 0.016 m, Reynolds No. 15800, wave velocity of 1301.8 m/s and valve closing time 0.02 sec.

The second comparison in Fig. 3 corresponds to experimental apparatus in [5] for a pipe of length 98.11 and a Reynolds No. of 15,800. As demonstrated in [1], the inverse frequency response agrees very well with the experimental data in [5]. In Fig. 3, the response decay rate and the primary mode frequency agree quite well.

As mentioned previously, the availability of experimental data is essentially limited to Reynolds numbers up to 15,800. Although it is not possible to totally verify results without experimental data, it is of the interest to compare the inverse frequency model with the MOC model at higher Reynolds numbers for smooth pipe. This is the objective of the next chapter.

Chapter 4

Evaluation of inverse frequency model for smooth pipe at relatively high Reynolds numbers.

In the previous chapter the MOC model formulated in this thesis was compared to the inverse frequency model [1] for relatively low Reynolds numbers out to 15800 corresponding to experimental data of previous researchers. The objective of this chapter is to compare the inverse frequency model for smooth pipe for Reynolds numbers up to 200,000.

Three sets of parameters are used. The first set of parameters has pipe length 98.11 m, diameter 0.016 m and wave velocity 1301.8 m/s. The second set of parameters has pipe length 4170 m, diameter 0.26 m and wave velocity 1210 m/s. The third set of parameters has pipe length 2500 m, diameter 0.1 m and wave velocity 1300 m/s.

The first comparison is shown in Fig. 4 for a Reynolds number of 25,000. As before, the grid size of the MOC is not small enough to accurately model the higher frequencies. The primary mode frequency compares quite well whereas the response decay rate is slightly different. Although not pursued in this thesis, it would be of interest to determine if a closer comparison is achieved with a larger value of n. Preliminary studies have revealed that the inverse frequency accuracy improves as the value of n is increased.

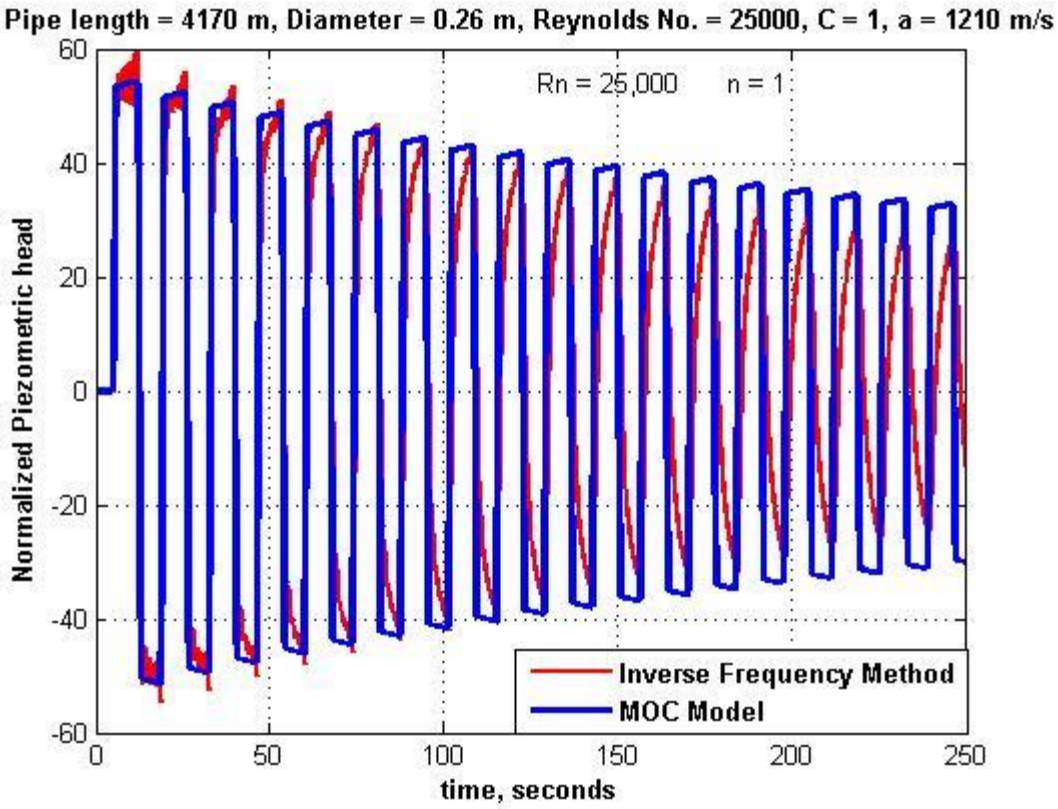

Figure 4. Comparing the response of the inverse frequency model [1] with the MOC response for pipe length 4170 m, diameter 0.260 m, Reynolds No. 25000, wave velocity of 1210 m/s and valve closing time 1 sec.

The second comparison is shown in Fig. 5 for a Reynolds number of 50,000. As before, the grid size of the MOC is not small enough to accurately model the higher frequencies. The primary mode frequency and the response decay rate agree quite well.

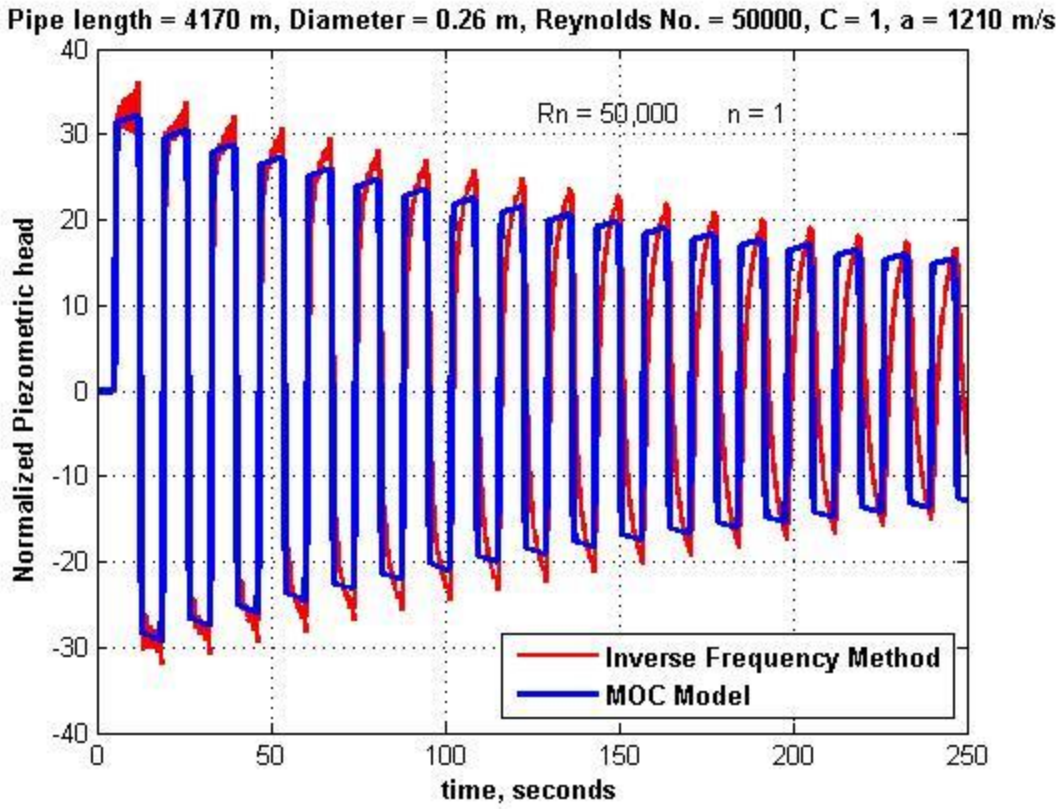

Figure 5.. Comparing the response of the inverse frequency model [1] with the MOC response for pipe length 4,170 m, diameter 0.260 m, Reynolds No. of 50,000, wave velocity of 1,210 m/s and valve closing time 1 sec.

The third comparison is shown in Fig. 6 for a Reynolds number of 100,000. As before, the grid size of the MOC is not small enough to accurately model the higher frequencies. The primary mode frequency compares quite well whereas the response decay rate is slightly different. It would be of interest to determine the effects of different values of n.

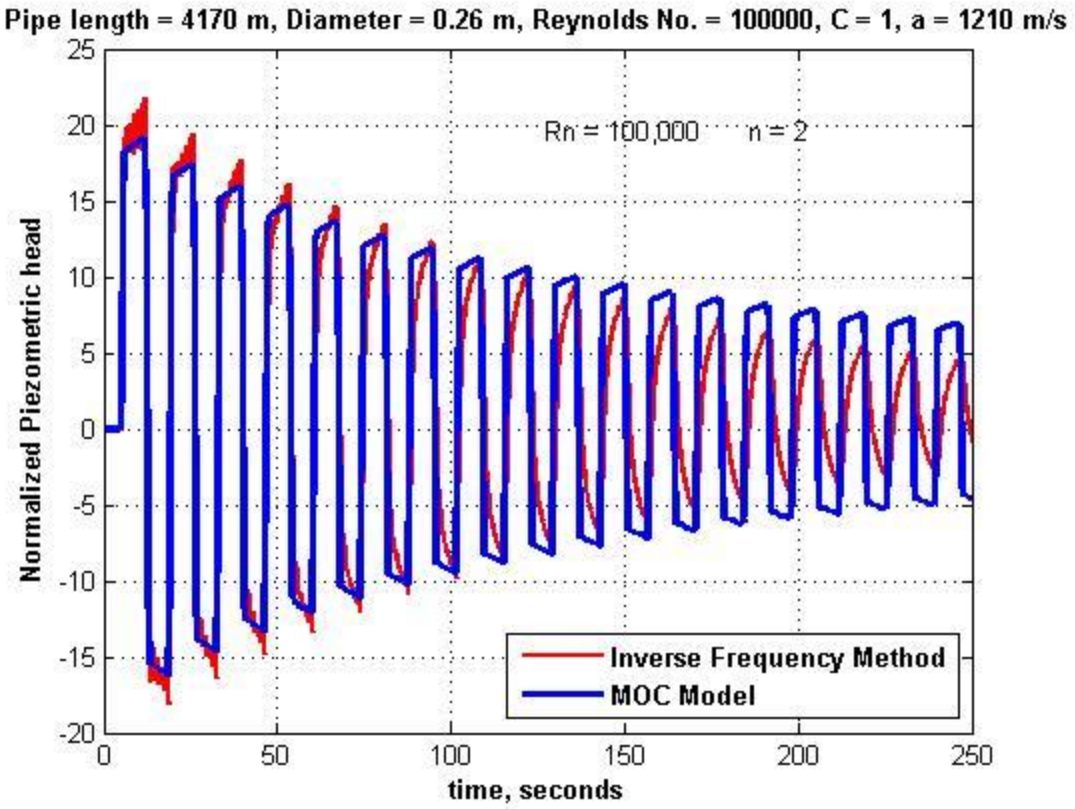

Figure 6. Comparing the response of the inverse frequency model [1] with the MOC response for pipe length 4,170 m, diameter 0.260 m, Reynolds No. 100,000, wave velocity of 1,210 m/s and valve closing time 1 sec.

The fourth comparison is shown in Fig. 7 for a Reynolds number of 200,000. As before, the grid size of the MOC is not small enough to accurately model the higher frequencies. The primary mode frequency compares quite well whereas the response decay rate is slightly different. As before, it would be of interest to determine the effects of different values of n.

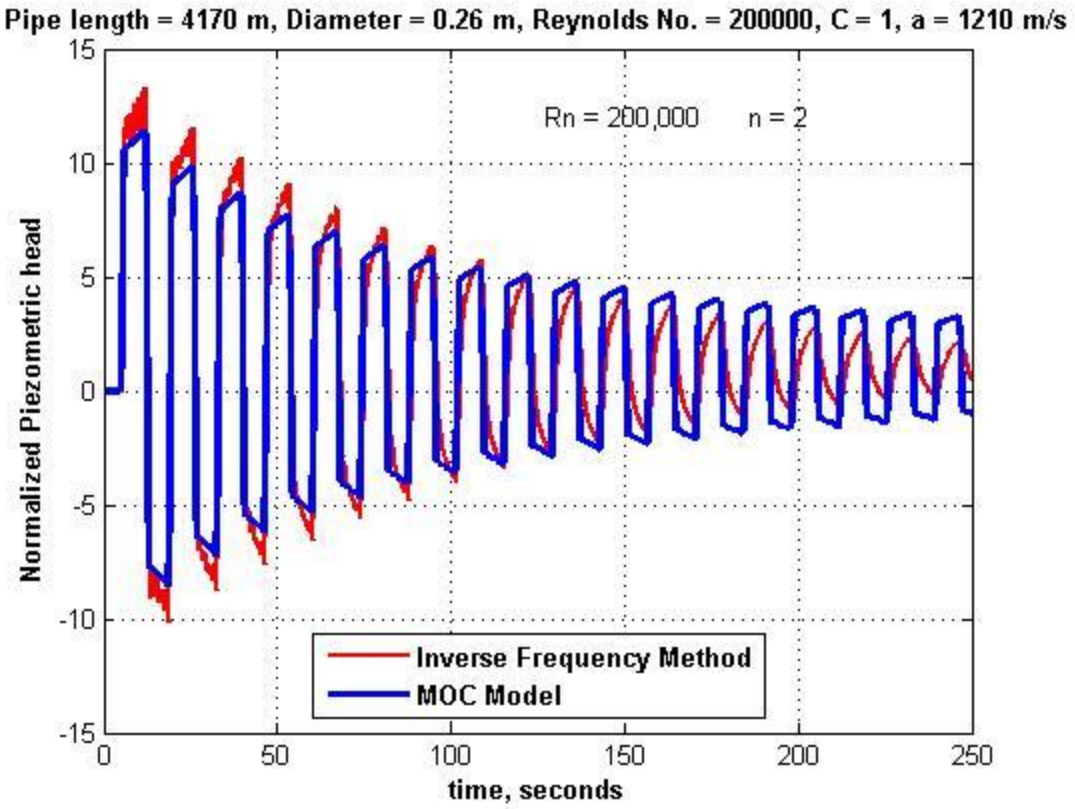

Figure 7.Comparing the response of the inverse frequency model [1] with the MOC response for pipe length 4,170 m, diameter 0.260 m, Reynolds No. 200,000, wave velocity of 1,210 m/s and valve closing time 1 sec.

The fifth comparison is shown in Fig. 8 for a Reynolds number of 25,000. As before, the grid size of the MOC is not small enough to accurately model the higher frequencies. The primary mode frequency compares quite well whereas the response decay rate is slightly different. As before, it would be of interest to determine the effects of different values of n.

The sixth comparison is shown in Fig. 9 for a Reynolds number of 50,000. As before, the grid size of the MOC is not small enough to accurately model the higher frequencies. The primary mode frequency compares quite well whereas the response decay rate is slightly different. As before, it would be of interest to determine the effects of different values of n.

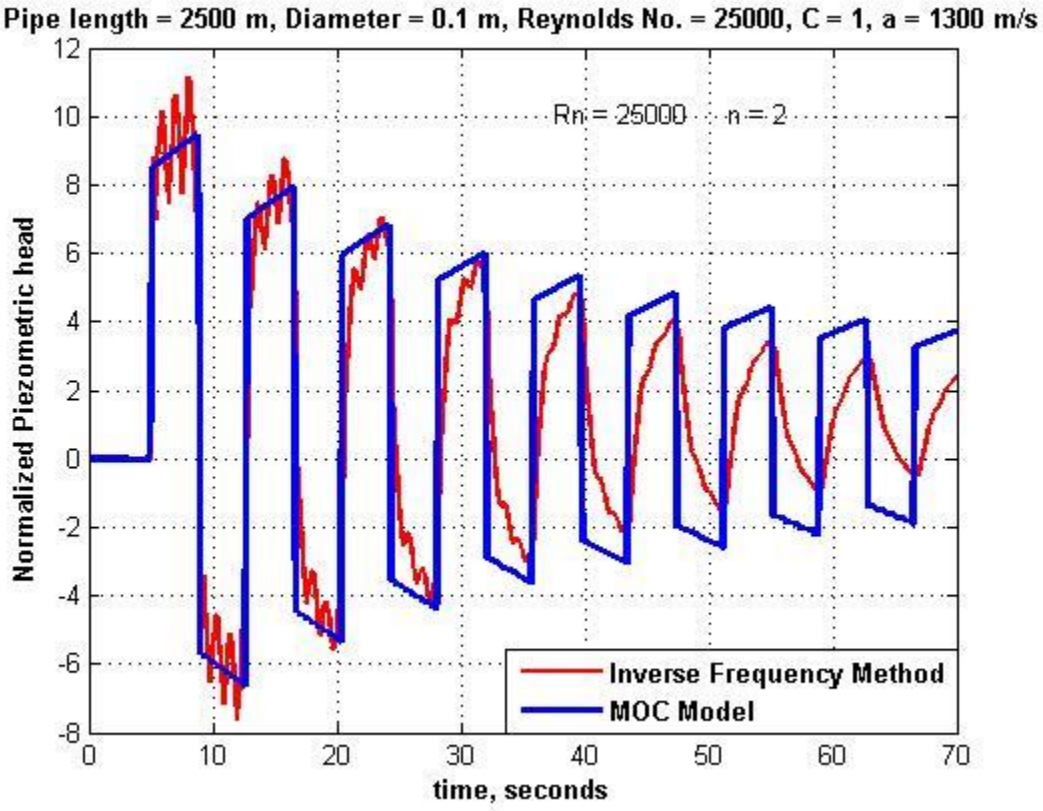

Figure 8. Comparing the response of the inverse frequency model [1] with the MOC response for pipe length 2,500 m, diameter 0.1 m, Reynolds No. 25,000, wave velocity of 1,300 m/s and valve closing time 0.1 sec.

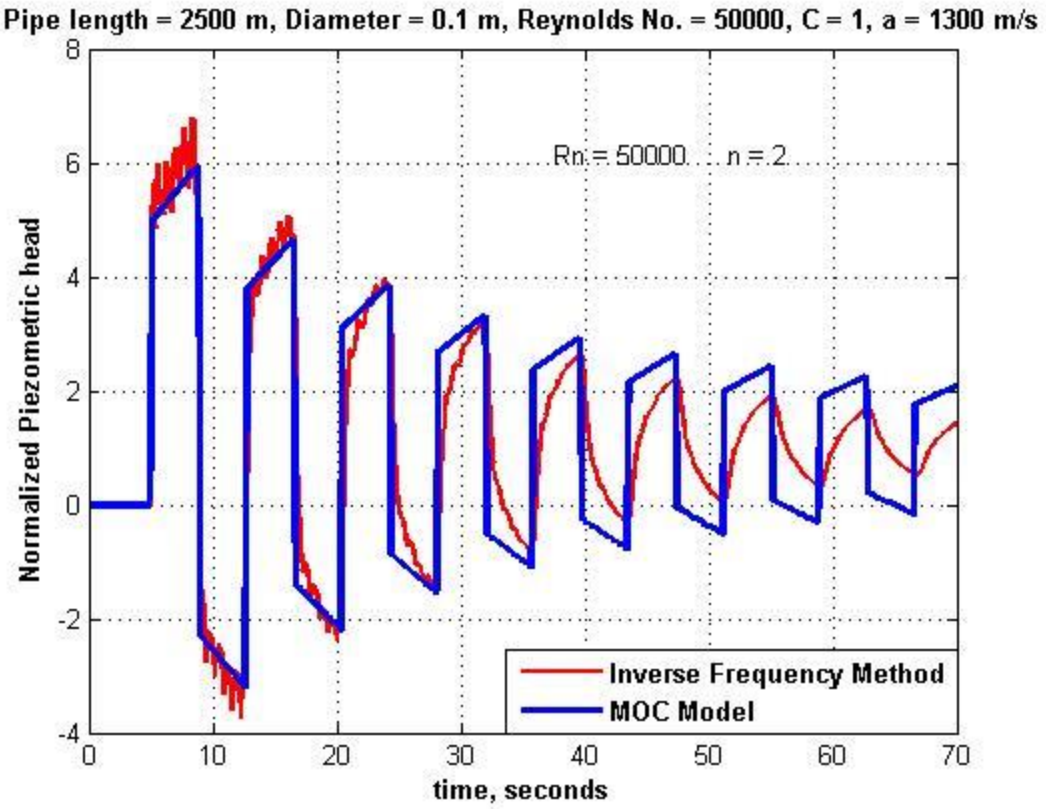

Figure 9. Comparing the response of the inverse frequency model [1] with the MOC response for pipe length 2,500 m, diameter 0.1 m, Reynolds No. 50,000, wave velocity of 1,300 m/s and valve closing time 0.1 sec.

The seventh comparison is shown in Fig. 10 for a Reynolds number of 100,000. As before, the grid size of the MOC is not small enough to accurately model the higher frequencies. The primary mode frequency compares quite well whereas the response decay rate is not the same. As before, it would be of interest to determine the effects of different values of n.

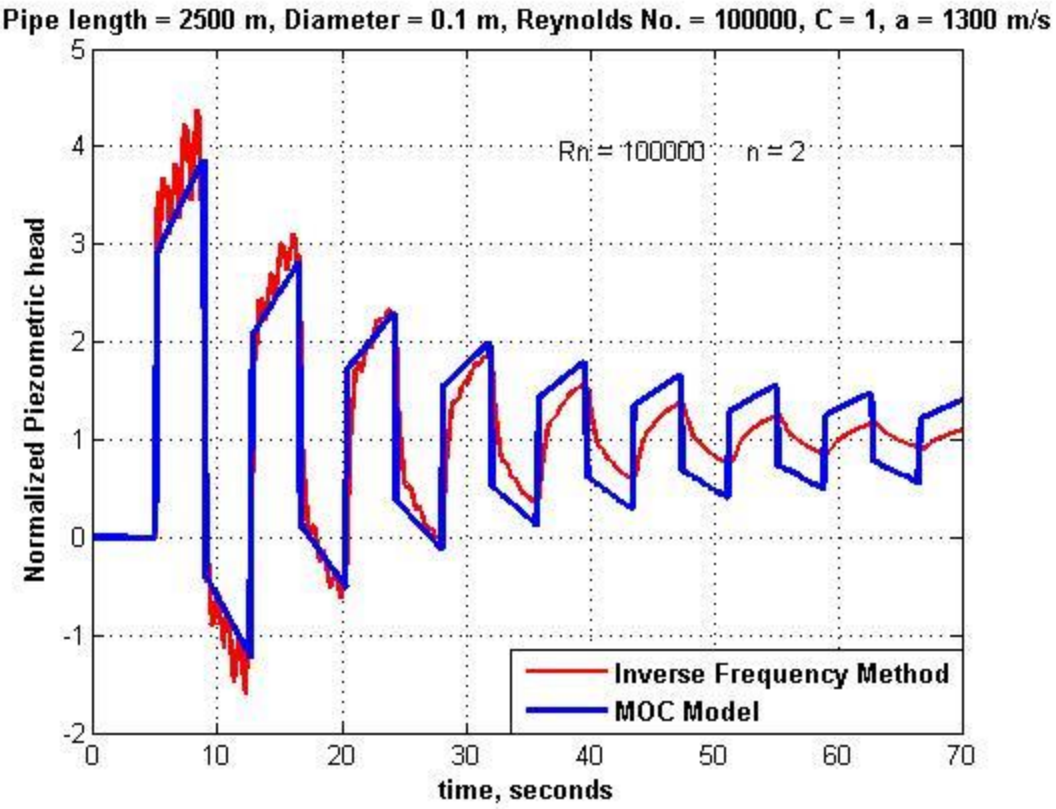

Figure 10. Comparing the response of the inverse frequency model [1] with the MOC response for pipe length 2,500 m, diameter 0.1 m, Reynolds No. 100,000, wave velocity of 1,300 m/s and valve closing time 0.1 sec.

The eight comparison is shown in Fig. 11 for a Reynolds number of 200,000. As before, the grid size of the MOC is not small enough to accurately model the higher frequencies. The primary mode frequency compares quite well whereas the response decay rate is not the same. As before, it would be of interest to determine the effects of different values of n.

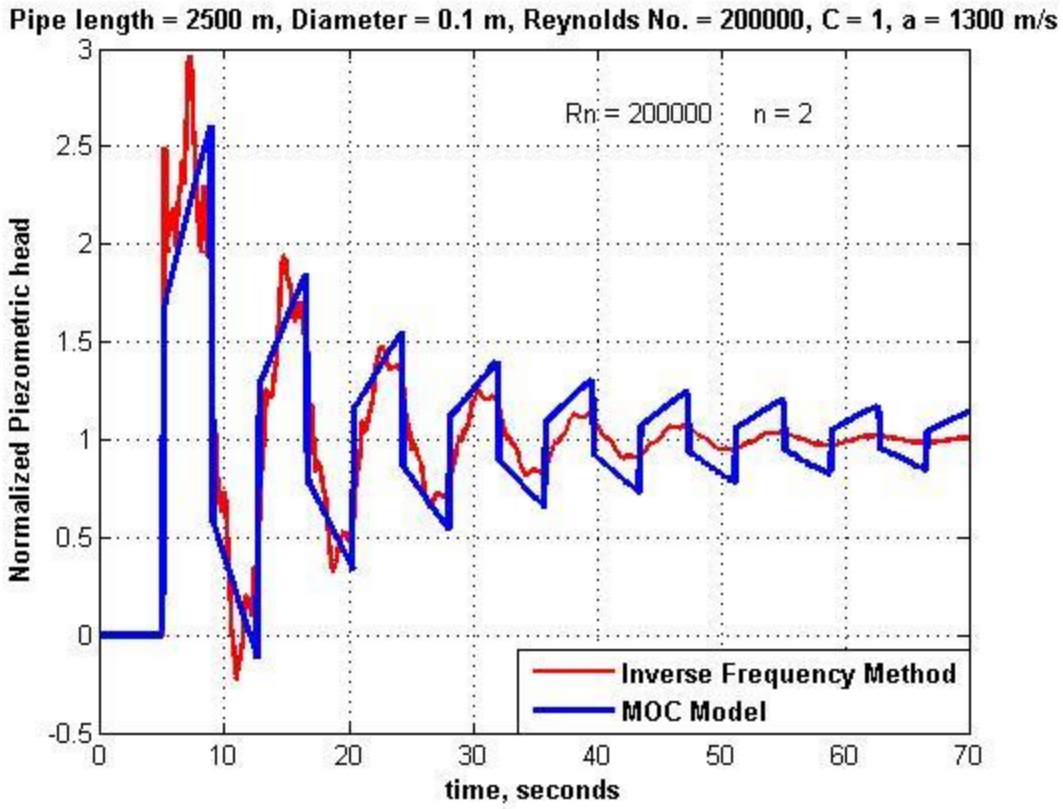

Figure 11. Comparing the response of the inverse frequency model [1] with the MOC response for pipe length 2,500 m, diameter 0.1 m, Reynolds No. 200,000, wave velocity of 1,300 m/s and valve closing time 0.1 sec.

Conclusion and Future work: The objective of this thesis is theoretical comparisons of the inverse frequency and MOC methods at higher Reynolds numbers for smooth pipe. The results revealed excellent agreement with the primary mode frequencies but discrepancies in the response decay rates at the higher Reynolds numbers. One of the reasons for these discrepancies might the Blasius friction factor used in the inverse frequency model; the Blasius friction is somewhat inaccurate for Reynolds numbers above 100,000. The Colebrook friction factor model, which is accurate to much larger Reynolds numbers, was used in the MOC method. Future work to study the effects of n is proposed. In addition, the availability of experimental data for higher Reynolds numbers would be most useful.

References

[1] Hullender, David A., 2016, “Alternative Approach for Modeling Transients in Smooth Pipe with Low Turbulent Flow,” ASME J. Fluids Eng., FE-16-1120.

[2] Stecki, J. S. and Davis, D. C., 1985, “Fluid Transmission Lines – Distributed parameter Models Part 1: A Review of the State of the Art,” Proc Instn Mech Eng, 200(4), pp. 215-228.

[3] Goodson, R. E. and Leonard, R. G., 1971, “A Survey of Modeling Techniques for Fluid Line Transients,” ASME 71-WA/FE-9.

[4] Zielke, W., 1968, “Frequency-Dependent Friction in Transient Pipe Plow”, Journal of Basic Engineering, 90(1), pp. 109-115.

[5] Adamkowski, A. and Lewandowski, M., 2006, “Experimental Examination of Unsteady Friction Models for Transient Pipe Flow Simulation,” ASME J Fluid Eng, 128(11), pp. 1351-1363.

[6] Brunone, B., Golia, U. M., and Greco, M., 1991, “Some Remarks on the Momentum Equation for Fast Transients,” International Meeting on Hydraulic Transients with Column Separation, 9th Round Table, IAHR, Valencia, Spain.

[7] Szymkiewicz, R. and Mitosek, M., 2014, “Alternative Convolution Approach to Friction in Unsteady Pipe Flow,” ASME J Fluid Eng 136(1).

[8] Vardy, A. E. and Brown, J. M. B., 2003, “Transient Turbulent Friction in Smooth Pipe Flows,” J of Sound and Vibration 259(5), pp. 1011-1036.

[9] Kagawa T., Lee I., Kitagawa A., Takenaka T., 1993, “High Speed and Accurate Computing of Frequency-Dependent Friction in Laminar Pipe Flow for Characteristics Method,” JSME, v49, 447, pp.2638-2644.

[10] Trikha A. K., 1975, “An Efficient Method for Simulating Frequency-Dependent Friction in Transient Liquid Flow,” ASME J. Fluids Eng., March , pp.97-105.

[11] Wylie, E.B., and Streeter, V.L., 1993, *Fluid Transients in Systems*, Prentice-Hall Inc. Englewood Cliffs, New Jersey, USA.

[12] Vítkovský, J.P., Stephens, M.L., Bergant, A., Simpson, A.R., and Lambert, M.F., 2004, "Efficient and accurate calculation of Vardy–Brown unsteady friction in pipe transients." *9th International Conference on Pressure Surges*, Chester, United Kingdom, March 24–26.

[13] Meniconi, S., Duan, H. F., Brunone, B., Ghidaoui, M. S., Lee, P. J., and Ferrante, M., 2014, “Further Developments in Rapidly Decelerating Turbulent Pipe Flow Modeling,” ASCE J Hydraulic Eng, 140(7).

[14] Soumelidis, M.I., Johnston, D.N., Edge, K.A., Tilley, D.G., 2005, “A Comparative Study of Modelling Techniques for Laminar Flow Transients in Hydraulic Pipelines,” Proceedings of the 6th JFPS International Symposium on Fluid Power, TSUKUBA, November 7-10.

[15] Didier Clamond (2008).Colebrook, MATLAB Central File Exchange. Retrieved May 4, 2016.

Appendix

For generating the graphs presented in the thesis, Part-A(MOC) and Part-B (inverse frequency method) mentioned below are used. In Part-A there are 4 M-files consisting of the main file, friction file, valve closing file, and Colebrook [15]. In part-B the M-file is for the inverse frequency model. In order to generate the graphs, first part-B is run and then part-A in order to compare the graphs.

Part -A

Main file

```
clc;
clear all;
global Ro Vct;
%% Exponential sum coefficients for Vardy-Brown weighting function
m=[5.03362 6.48760 10.7735 19.9040 37.4754 70.7117 133.460 251.933
476.597 932.860];
m=m';
ni=[4.78793 51.0897 210.868 765.030 2731.01 9731.44 34668.5 123511 440374
1590300];
ni=ni';
%% Input Parameters
L=2500;%length of pipe
d=0.1;%diameter of pipe
```

```
rho=1000;%Density
nu=2e-6;%Kinematic Viscoscity
a=1300;%wave speed
re=25000;% Reynolds no
E=2.2e-03;%Roughness
C=1;
Vct=0.1;% Valve Closing time
Cv=1-C;
%Ro=E/d;
Ro=0;% Roughness Coefficeint
Vo=re*nu/d;
mju=2e-3;
f=colebrook(re,Ro); %Colebrook Friction factor
Po=(f*L*rho*Vo^2)/(2*d);

%% MOC Grid Creation
n=100;h=L/(n-1);V(1:n)=Vo;P(1:n)=Po;
dt=h/a;tmax=70;itmax=tmax/dt;
for i=2:n
    P(i)=P(i-1)-f*rho*Vo^2*h/(2*d);
end
%% Calculation of Friction terms
```

```
A=sqrt(1/4*pi);ki=re^(-0.0567);k=log10(15.29*ki);B=((re)^k)/12.86;% smooth pipe
E=2.2e-03;%Roughnes in pipe
%A=0.0103*sqrt(re)*(Ro)^0.39;B=0.352*re*(Ro)^0.41;% Rough pipe
delt=4*nu*dt/d^2;
sum=0;
for k=1:10
   sum=sum+(A*m(k))*(exp(-(ni(k)+B)*delt));
end
lambda=(16*nu*sum*h)/(a*d^2);

%% Calculation of Velocities and Presussre at evry point as Per MOC-Grid

for it=1:itmax
   t=it*dt;
   for i=2:n-1
      Pa=P(i-1);Pb=P(i+1);Va=V(i-1);Vb=V(i+1);
      Fa=Friction(Va,d,nu);
      Fb=Friction(Vb,d,nu);
      Ea=Fa*rho*h/(2*a*d)*Va*abs(Va);
      Eb=Fb*rho*h/(2*a*d)*Vb*abs(Vb);
      Pc(i)=a/2*((Pa+Pb)/a+rho*(Va-Vb)+(Eb-Ea));
      Vc(i)=0.5*(((Pa-Pb)/a)+rho*(Va+Vb)-Eb-Ea)/(rho+lambda);
```

```
    end
    Pc(1)=Po;
    Vb=V(2);Pb=P(2);
    Fb=Friction(Vb,d,nu);
    Eb=Fb*h/(2*a*d)*Vb*abs(Vb);
    Vc(1)=(rho*Vb+(Pc(1)-Pb)/(a)-rho*Eb)/(rho+lambda);
    Vc(n)=Vo*VctFunctn(t);
    Va=V(n-1);Pa=P(n-1);
    Fa=Friction(Va,d,nu);
    Pc(n)=(Pa-(rho+lambda)*a*Vc(n) + rho*a*Va - a*Ea);
    vmatrix(it,1:n)=Vc(1:n);
    pmatrix(it,1:n)=Pc(1:n);
    P=Pc;V=Vc;
end
%% Plotting of Graphs
hold on
time=linspace(0,tmax,itmax);
Pressure=((pmatrix(:,n))/Po);
plot(time,Pressure,'linewidth',2.5)
% plot(time,(vres(:,n)),'linewidth',2.5);
legend('\bfInverse Frequency Method','\bfMOC Model','Location','Best')
xlabel('\bftime, seconds')
```

```
ylabel('\bfNormalized Piezometric head')
title(['\bfPipe length = ' num2str(L) ' m, ' '\bfDiameter = ' num2str(d) ' m, '
'\bfReynolds No. = ' num2str(re) ', ' '\bfC = ' num2str(C) ', ' '\bfa = ' num2str(a) '
m/s'])
```

M-File for Calculating Friction

```
function f=Friction(V,d,nu)
global  Ro

re=abs(V)*d/nu;
if re<2100
   f=64/re;
else
   f=colebrook(re,Ro);
end
```

Colebrook.m [15]

```
function F = colebrook(R,K)
% F = COLEBROOK(R,K) fast, accurate and robust computation of the
%     Darcy-Weisbach friction factor F according to the Colebrook equation:
%                          -                    -
```

```
%     1                  |   K       2.51       |
%  ---------  =  -2 * Log_10 |  ----- + -------------  |
%   sqrt(F)               |   3.7     R * sqrt(F)   |
%                         -                       -
% INPUT:
%   R : Reynolds' number (should be >= 2300).
%   K : Equivalent sand roughness height divided by the hydraulic
%       diameter (default K=0).
%
% OUTPUT:
%   F : Friction factor.
%
% FORMAT:
%   R, K and F are either scalars or compatible arrays.
%
% ACCURACY:
%   Around machine precision forall R > 3 and forall 0 <= K,
%   i.e. forall values of physical interest.
%
% EXAMPLE: F = colebrook([3e3,7e5,1e100],0.01)
%
% Edit the m-file for more details.
```

```
% Method: Quartic iterations.
% Reference: http://arxiv.org/abs/0810.5564
% Read this reference to understand the method and to modify the code.

% Author: D. Clamond, 2008-09-16.

% Check for errors.
if any(R(:)<2300) == 1,
  warning('The Colebrook equation is valid for Reynolds'' numbers >= 2300.');
end,
if nargin == 1 || isempty(K) == 1,
  K = 0;
end,
if any(K(:)<0) == 1,
  warning('The relative sand roughness must be non-negative.');
end,

% Initialization.
X1 = K .* R * 0.123968186335417556;          % X1 <- K * R * log(10) / 18.574.
X2 = log(R) - 0.779397488455682028;          % X2 <- log( R * log(10) / 5.02 );
```

```
% Initial guess.
F = X2 - 0.2;

% First iteration.
E = ( log(X1+F) - 0.2 ) ./ ( 1 + X1 + F );
F = F - (1+X1+F+0.5*E) .* E .*(X1+F) ./ (1+X1+F+E.*(1+E/3));

% Second iteration (remove the next two lines for moderate accuracy).
E = ( log(X1+F) + F - X2 ) ./ ( 1 + X1 + F );
F = F - (1+X1+F+0.5*E) .* E .*(X1+F) ./ (1+X1+F+E.*(1+E/3));

% Finalized solution.
F = 1.151292546497022842 ./ F;          % F <- 0.5 * log(10) / F;
F = F .* F;                             % F <- Friction factor.
```

M-File for Valve closure

```
function Vr=VctFunctn(t)
global Vct
ts=0.3;
if t>=ts+Vct
    Vr=3e-304;
 else
```

```
    if (t>ts && t<ts+Vct)
        Vr=0.5+0.5*cos(pi*(t-ts)/Vct);
    else
       Vr=1;
   end
end


end
```

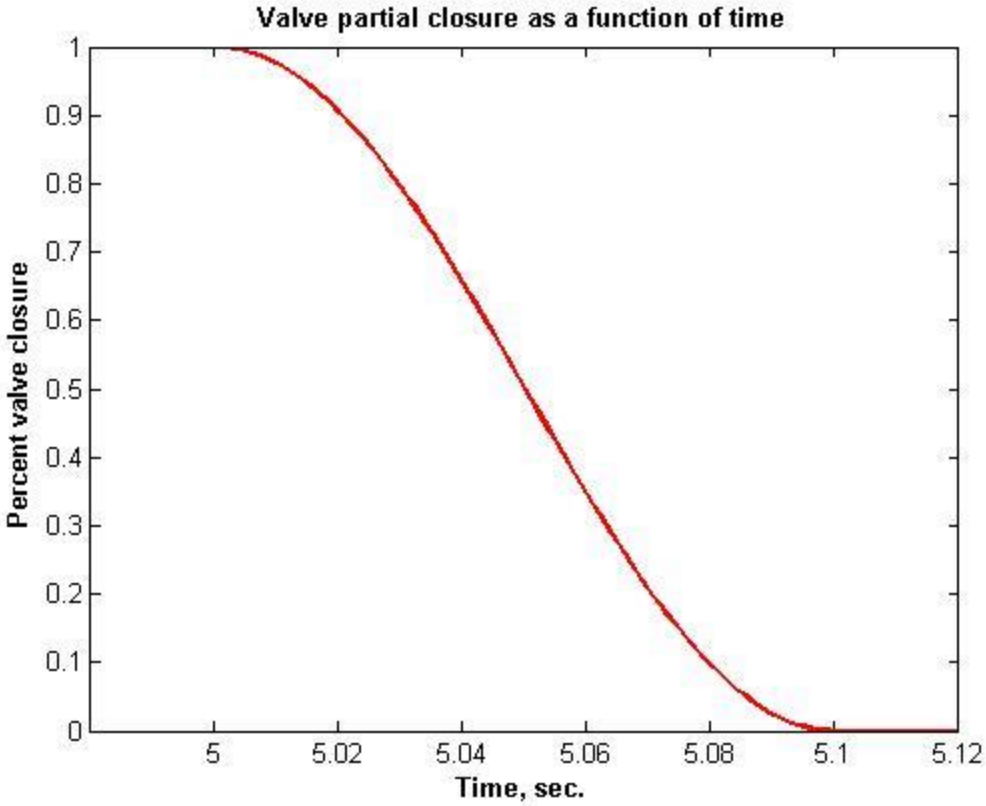

Figure 12. Valve Closing Curve

The Figure.12 shows the nature of curve for valve closing, various valve closing times have been used in these thesis but nature of graphs remains the same.

Part-B

```
function Rn15800Cv_6_21_16%(S1,S2,V1,V2)
warning off
format shortg

% Required inputs; you will have to guess the order, wmax, and wmin at first until
% you see the frequency response and decipher the necessary frequency range
dorder=21;
wmin=1.e-8;wmax=22000;wminplot=100;wmaxplot=1.25*wmax;
Cv=1;%   0 < Cv <= 1

norder=dorder-1;
nd=ceil(log10(wmax)-log10(wmin));%Determines the number of decades in the
frequency range and rounds up to the next integer
w=logspace(log10(wmin),log10(wmax),1000*nd);%Generates at least 1000
points per decade
Lw=length(w);
for k=1:Lw
s(k)=w(k)*1i;
[H(k)]=WaterHammerTF(s(k));
end
```

```
wt=ones(1,Lw);%weighting terms for curve fit
[numa,dena]=invfreqs(H,w,norder,dorder,wt,100);%curve fitting with 100 attempts if necessary
Gapprox=tf(numa,dena);%linear transfer function approximation from curve fitting frequency response
damp(Gapprox)%gives eigenvalues of the transfer function
DCGain=dcgain(Gapprox)% comparing the dcgain of the approximation and the original transfer functions
% helps to determine if wmin was low enough
%
% Generate Freq. Resp. plots to determine the accuracy of curve fit.
if wminplot>=wmaxplot, error('wmin is too small; very low non-resonant peaks are messing up the calcualtions. Increase wmin and try again.'),end;
ndp=ceil(log10(wmaxplot)-log10(wminplot));%Determines the number of decades in the plotting frequency range and rounds up to the next integer
wp=logspace(log10(wminplot),log10(wmaxplot),500*ndp);%Generates at least 100 points per decade for the plots
Lwp=length(wp);
Hc=freqs(numa,dena,wp);%generates frequency response of the computed transfer function
MHc=20*log10(abs(Hc));%magnitudes of the frequency response in dB
AHc=angle(Hc)*180/pi;%angles of the frequency response in degrees
```

```
clear H s

% recompute the original function with same frequencies used for the transfer
function approximation
for k=1:Lwp
s(k)=wp(k)*1i;
[H(k)]=WaterHammerTF(s(k));
end
MH=20*log10(abs(H));
AH=angle(H)*180/pi;

Figureure(1)
semilogx(wp,AH,'k',wp,AHc,'r:','LineWidth',2)
title('Phase Angle Comparison Plots')
%xlabel('Frequency, rad/sec');ylabel(' Phase Angle, degrees');
xlabel('Normalized frequency \omega/\omega_v ')
ylabel('Phase Angle, degrees')
legend('Original funcition','Approximation','Location','Best')
grid on
grid minor

Figureure(2)
```

```
semilogx(wp,MH,'k',wp,MHc,'r:','LineWidth',2)
xlabel('Normalized frequency \omega/\omega_v ')
ylabel('Normalized transfer function magnitude,   ( \DeltaP_b/P_e)/ (
\DeltaQ_b/Q_e) dB')
legend('Original function','Approximation','Location','Best')
title('Magnitude Comparison Plots')
grid on
grid minor

Figureure(3)
[ynorm,tnorm]=step(Cv*Gapprox,0.06);% to shorten the normalized simulation
time to FT, step(Gapprox,FT)
plot(tnorm,ynorm,'r','LineWidth',2)
grid
TEXT=[RN,NN];
text(0.5*max(tnorm),0.97*max(ynorm),TEXT)
title('Wate hammer normalized pressure pulsations for instant partial closure')
ylabel('Normalized pressure at valve end of pipe   \DeltaP_b/P_e')
xlabel('Normalized time t\omega_v')

clear t Y
Y=ynorm*Pe/(den*9.8);t=tnorm*r^2/kvis;
```

```
Figureure(4)
plot(t,Y,'r:','Linewidth',2)
grid on;
text(0.5*max(t),0.9*max(Y),TEXT)
xlabel('time, seconds')
ylabel('Pressure at valve (piezometric head, m)')
title('L=98.11 m, D=0.016 m, a=1301.8 m/s, valve partially closed instantly')

VCT=0.1;       % Valve close time in seconds.

for nt=1:length(t)% generate shaped valve closing
    if t(nt)<=VCT
        u(nt)=.5+0.5*cos(pi*(t(nt)/VCT-1));end
     if t(nt)>VCT
        u(nt)=1;end
end
u=Cv*u;% 0 < Cv <=1

Figureure(5)
plot(t,u*100,'r','LineWidth',2)
grid
xlabel('time, sec.')
```

```
ylabel('percent valve closure')
title('valve partial closure as a function of time')
axis([0 1.2*VCT -10 110])

Figureure(6)
tnorm=t*kvis/r^2;% need normalized time since Gapprox corresponds to
normalized time
[YS,T]=lsim(Gapprox,u,tnorm);
plot(T,YS,'r','LineWidth',2)
grid
text(0.5*max(T),0.9*max(YS),TEXT)
xlabel('normalized time, sec.')
ylabel('Normalized pressure at valve end of pipe   \DeltaP_b/P_e')
title('L=98.11 m, D=0.016 m, a=1301.8 m/s, valve partial close time 0.02 sec')

Figureure(7)
plot(5+T*r^2/kvis,YS,'r','LineWidth',2)% replot using un-normalized time, sec
grid
text(0.5*max(T*r^2/kvis),0.9*max(YS),TEXT)
xlabel('time, sec.')
ylabel('Normalized pressure at valve end of pipe   \DeltaP_b/P_e')
title('L=98.11 m, D=0.016 m, a=1301.8 m/s, valve partial close time 0.02 sec')
```

```
PE=Pe/(den*9.8)
xlim([0 70]);
  function [H]=WaterHammerTF( s )

     den=1000;a=1300;kvis=2e-6;
      r=0.05;L=2500;

      Rn=25000;
      RN='Rn = 25000     ';

      Qe=Rn*pi*kvis*r/2;
      absvis=kvis*den;
      Pe=0.2414*(den^0.75)*(absvis^0.25)*L*(Qe^1.75)/(2*r)^4.75;

      Dn=kvis*L/(a*r^2)
       B=2*besselj(1,j*sqrt(s))/(j*sqrt(s).*besselj(0,j*sqrt(s)));
       sqr=sqrt(1-B);
       RTOZ=0;n=2;g=Dn*s/sqr;%This is the case for laminar flow, Rn<1187.6
       NN='laminar flow';
        if Rn>=1187.6
```

```
        n=2;%Desired number of segments in turbulence model. May need to be
increased for larger values of Dn
        NN='n = 2';

        RTOZ=Dn*sqr*(0.039544*Rn^0.75-8);
         g=Dn*s/(n*sqr);% gamma
        end

       W(1,1)=cosh(g)+RTOZ*sinh(g)/n;
       W(1,2)=-(sinh(g)+RTOZ*cosh(g)/n)/(8*Dn*sqr+RTOZ);
       W(2,1)=-(8*Dn*sqr+RTOZ)*sinh(g);
      W(2,2)=cosh(g);
       X=W^n;

       H=-X(1,2)/X(2,2);% this is the transfer function for a negative unit step
    end

end
```

k	n_k^*	m_k^*	τ_{mk}
1	4.78793	5.03362	-
2	51.0897	6.48760	3.20×10^{-2}
3	210.868	10.7735	8.70×10^{-3}
4	765.030	19.9040	2.44×10^{-3}
5	2731.01	37.4754	6.84×10^{-4}
6	9731.44	70.7117	1.92×10^{-4}
7	34668.5	133.460	5.39×10^{-5}
8	123511	251.933	1.51×10^{-5}
9	440374	476.597	4.20×10^{-6}
10	1590300	932.860	1.02×10^{-6}

Table 1. Best fit exponential sum coefficients for Vardy-Brown weighting function [12]

As noted in [12], to use these coefficients properly, the following condition needs to be followed: $\Delta\tau > \tau_{mk}$.

Biographical Information

Mohammad Saifullah, completed his undergraduate studies from Mumbai University, India. His undergraduate project was based on Renewable energy. He worked as a lecturer at Thakur polytechnic, Mumbai. Later he came to UTA for his master's Program where his interest was focused on Controls and Automation. His aims to become and industrial Automation engineer.